Supplementary Materials: A Sequential Algorithm to Detect Diffusion Switching along Intracellular Particle Trajectories

V. Briane [1 2], M. Vimond [2], C.A.V Cruz [3], +XXXX, A. Salomon [1] and C. Kervrann [1]

[1]INRIA, Centre de Rennes Bretagne Atlantique, Serpico Project-Team, Rennes, 35042, France

[2]CREST (Ensai, Université Bretagne Loire), Bruz, 35170, France

[3]Institut Curie, 25 Rue d'Ulm, 75005 Paris, France.

1 A Change-Point Model

In this section, we describe a more general change-point model that includes the model presented in Section 2.1 of the paper. As our sequential algorithm is based on the test procedure of Briane et al. (2018), we consider a similar diffusion process as in Briane et al. (2018) adapted for the change-point problem :

$$dX_t = \mu(X_t, t)dt + \sigma(t)dB_t^{\mathfrak{h}(t)}, \qquad t \in [t_0, t_{n-1}], \tag{1.1}$$

where $B^{\mathfrak{h}(t)}$ denotes a $d-$dimensional fractional Brownian motion of Hurst parameter $\mathfrak{h}(t)$; the unknown parameters of the model are the Hurst parameter function $\mathfrak{h} : \mathbb{R}^+ \to (0, 1)$, the diffusion coefficient function $\sigma : \mathbb{R}^+ \to (0, \infty)$ and the drift term $\mu : \mathbb{R}^d \times \mathbb{R}^+ \to \mathbb{R}^d$. Compared to the model presented in Section 2.1, we add the Hurst parameter $\mathfrak{h}(t)$: when $\mathfrak{h} \neq 1/2$ the SDE (1.1) is driven by fractional Brownian motion $B^{\mathfrak{h}(t)}$ which has correlated increments. Also, in model (1.1), we assume that the diffusion coefficient σ can vary over time while this parameter is constant in the model of the paper.

As before we suppose that the parameters defining the diffusion (1.1) are piecewise constant over time. Then, we assume that there exists a sequence of N change-points on $[t_0, t_{n-1}]$, namely $t_0 = \tau_0 < \tau_1 < \dots \tau_N < \tau_{N+1} = t_{n-1}$ such that,

$$\mu(x,t) = \mu_j(x),\ \mathfrak{h}(t) = \mathfrak{h}_j,\ \sigma(t) = \sigma_j \text{ for } t \in [\tau_j, \tau_{j+1}). \tag{1.2}$$

The unknown parameters of the model are the vector of change-points $(\tau_j)_{j=1\dots N}$, the number of change-points N, and the parameters $(\mathfrak{h}_j, \mu_j, \sigma_j)$ of the diffusion process restricted on subinterval $[\tau_j, \tau_{j+1})$. The drift term μ_j is assumed to satisfy the usual Lipschitz and linear growth conditions in order that the SDE (1.1) admits a strong solution on $[\tau_j, \tau_{j+1})$ (see (Nualart & Ouknine 2002) for $0 < \mathfrak{h} \leq 1/2$ and (Mishura 2008) for $1/2 < \mathfrak{h} < 1$). We extend by continuity the solution on each subinterval to get a solution on $[t_0, t_{n-1}]$.

Again we assume that for each τ_j there exists $0 \leq j^\star \leq n$ such that $\tau_j = t_{j^*}$ (the change of motion occurs precisely at a sampling time). In analogy with the model of the paper, we assume that $(\mathfrak{h}_j, \mu_j)$ and $(\mathfrak{h}_{j+1}, \mu_{j+1})$ are associated to different types of diffusion (Brownian motion, subdiffusion or superdiffusion). We note that the parameter σ_j does not influence the type of diffusion.

Finally we have to mention that the test procedure of Briane et al. (2018) has also been validated in the case of continuous time random walk (CTRW) characterized by a subdiffusive behaviour. CTRW are not defined through stochastic differential equations. Then, our sequential algorithm can deal with an even greater variety of change-point models than the two presented here (for instance transition of motion including CTRW).

1.1 Choice of the cut-off value (γ_1, γ_2) in Procedure 1 Ideally, γ_1 and γ_2 are choosen such that we control the type I error at level $0 < \alpha < 1$; in other words such that we control the probability to detect falsely a change-point when the trajectory is fully Brownian. Then, controlling the type I error at level $0 < \alpha < 1$ is equivalent to have :

$$P_{H_0}\left(\exists i \in \{k, \dots, n^\star\},\quad \sum_{j=i}^{i+c-1} Q_j \geq pc\right) \leq \alpha, \tag{1.3}$$

where $n^\star = n - k - c + 1$ and P_{H_0} is the probability under H_0, that is under the hypothesis that the trajectory is fully Brownian. In fact, the left hand side of Equation (1.3) is the probability to build one cluster of minimal size c under H_0, when clusters are defined thanks to Eq. (3.3) (see step 2 of Procedure 1). Then, controlling the probability in (1.3) at level α under H_0 is equivalent to control the probability to detect falsely a change-point under H_0 at level α (definition of the type I error).

Proposition 1. *Let define* $d_i = \min(B_i, A_i)$ *and* $D_i = \max(B_i, A_i)$ *where* A_i *and* B_i *are the test statistics (3.1), for* $i = k, \dots, n^\star$. *We define* $\gamma_1^\star$ *and* $\gamma_2^\star$ *as:*

$$\begin{aligned} P_{H_0}\Big(\min_{i=k,\dots,n^\star} d_{i(\lceil pc/2 \rceil)} < \gamma_1^\star\Big) &= \frac{\alpha}{2}, \\ P_{H_0}\Big(\max_{i=k,\dots,n^\star} D_{i(c-\lceil pc/2 \rceil)} > \gamma_2^\star\Big) &= \frac{\alpha}{2}, \end{aligned} \tag{1.4}$$

where,

- $d_{i(\lceil pc/2 \rceil)}$ *is the* $\lceil pc/2 \rceil$ *smallest element of* $(d_i, \dots, d_{i+c-1})$,
- $D_{i(c-\lceil pc/2 \rceil)}$ *the* $c - \lceil pc/2 \rceil$ *smallest element of* $(D_i, \dots, D_{i+c-1})$ *(equivalently the* $\lceil pc/2 \rceil$ *greatest element).*

In other words, $\gamma_1^\star$ *is the quantile of order* $\alpha/2$ *of the random variable* $\min_{i=k,\dots,n^\star} d_{i(\lceil pc/2 \rceil)}$ *and* $\gamma_2^\star$ *is the quantile of order* $1-\alpha/2$ *of the random variable* $\max_{i=k,\dots,n^\star} D_{i(c-\lceil pc/2 \rceil)}$. *With the choice of cut-off values* $\gamma_1^\star$ *and* $\gamma_2^\star$ *Procedure 1 with parameters* (k, c, p) *controls the type I error (1.3) at level* α.

Proposition 1 provides a choice for γ_1 and γ_2 in order to control the level of the procedure. These thresholds $\gamma_1^\star$ and $\gamma_2^\star$ can be approximated by Monte Carlo estimate, see Algorithm 1. A proof of Proposition 1 is available in Section 1.2. Nethertheless this choice is too conservative as it is shown in Table 1. This fact is not surprising since the bound in Equation (1.11) is loose in the proof of Proposition 1.

We investigate another choice by Monte Carlo experiments, and we recommend to use the heuristic cut-off values $(\tilde{\gamma}_1, \tilde{\gamma}_2)$ defined as follow :

$$\begin{aligned} P_{H_0}\Big(\min_{i=k,\dots,n^\star} d_{i(\lceil pc \rceil)} < \tilde{\gamma}_1\Big) &= \frac{\alpha}{2}, \\ P_{H_0}\Big(\max_{i=k,\dots,n^\star} D_{i(c-\lceil pc \rceil)} > \tilde{\gamma}_2\Big) &= \frac{\alpha}{2}. \end{aligned} \tag{1.5}$$

Notice that we replace $pc/2$ in Equation (1.4) by pc. Then, it is straightforward to show that $\gamma_1^\star \leq \tilde{\gamma}_1$ and $\gamma_2^\star \geq \tilde{\gamma}_2$. As a consequence, Procedure 1 with $(\tilde{\gamma}_1, \tilde{\gamma}_2)$ is less conservative than with $(\gamma_1^\star, \gamma_2^\star)$. In other words, Procedure 1 is more sensitive to the presence of subdiffusion or superdiffusion with $(\tilde{\gamma}_1, \tilde{\gamma}_2)$ than with $(\gamma_1^\star, \gamma_2^\star)$. Moreover Table 1 illustrates that the Monte Carlo estimates of the type I error rate is very closed to the expected value $\alpha = 5\%$ whatever the values of n and k. As $(\tilde{\gamma}_1, \tilde{\gamma}_2)$ are both controlling the type I error rate and are more sensitive to detect subdiffusion and superdiffusion, they are naturally preferred to $(\gamma_1^\star \gamma_2^\star)$. Table 2 gives Monte Carlo approximations of $(\gamma_1^\star, \gamma_2^\star)$ and $(\tilde{\gamma}_1, \tilde{\gamma}_2)$ as an illustration.

Table 1: Monte Carlo estimates of the type I error rates (in percentage) of Procedure 1 for different choices of the cut-off values (γ_1, γ_2) when $\alpha = 5\%$ and $(c, p) = (k/2, 0.75)$. The number of Monte Carlo replications is 100 001 to get a standard deviation around $\pm 0.14\%$ of the Monte Carlo estimates.

		Probability of Type I error	
n	k	with $(\gamma_1^\star, \gamma_2^\star)$	with $(\tilde{\gamma}_1, \tilde{\gamma}_2)$
150	20	0.60	5.21
150	30	0.65	4.81
150	40	0.94	4.56
300	20	0.47	5.04
300	30	0.59	4.89
300	40	0.82	4.83

Table 2: Cut-off values (γ_1, γ_2) of Procedure 1 at level $\alpha = 5\%$ defined in Equation (2.2) and (2.3) according the trajectory sizes n and window size k for dimension $\mathrm{d} = 2$. We use Monte Carlo experiments over 10 001 replications and the default parameters $(c, p) = (k/2, 0.75)$.

n	k	$\gamma_1^\star$	$\gamma_2^\star$	$\tilde{\gamma}_1$	$\tilde{\gamma}_2$
150	20	0.61	3.38	0.74	3.12
150	30	0.65	3.35	0.79	3.09
150	40	0.68	3.28	0.81	3.05
300	20	0.58	3.55	0.71	3.29
300	30	0.62	3.55	0.74	3.28
300	40	0.64	3.52	0.75	3.27

Remark 1.1. *We note that the cut-off values defined by (1.4) or (1.5) potentially depend on the diffusion coefficient σ (and on the step of time Δ). In fact, the null hypothesis H_0 depends on parameter σ (and Δ). However, the test statistics (3.1) do not depend on (σ, Δ) under H_0. Consequently, the cut-off values defined by (1.4) or (1.5) neither depend on (σ, Δ).*

1.2 Proof of Proposition 1

Proof. We suppose that the trajectory $\mathbb{X}_n$ is generated under the null hypothesis (3.2) that is the trajectory is fully Brownian. For simplicity, we note P the probability under H_0 (noted P_{H_0} previously).We want to show that under H_0, Procedure 1 with thresholds γ_1

and γ_2 defined in Proposition 1, controls the probability of the type I error at level α:

$$P\left(\exists i \in \{k, \dots, n^\star\}, \quad \sum_{j=i}^{i+c-1} Q_j \geq pc\right) \leq \alpha \tag{1.6}$$

where $n^\star = n - k - c + 1$.
We express the event $\{Q_i = 1\}$ as:

$$\begin{aligned}\{Q_i = 1\} = &\{\gamma_1 \leq B_i \leq \gamma_2, A_i < \gamma_1\} \cup \{\gamma_1 \leq B_i \leq \gamma_2, A_i > \gamma_2\} \\ &\cup \{B_i < \gamma_1, \gamma_1 \leq A_i \leq \gamma_2\} \cup \{B_i > \gamma_2, \gamma_1 \leq A_i \leq \gamma_2\} \\ &\cup \{B_i < \gamma_1, A_i > \gamma_2\} \cup \{B_i > \gamma_2, A_i < \gamma_1\}\end{aligned} \tag{1.7}$$

Then we deduce the following :

$$\begin{aligned}\{Q_i = 1\} &\subset \{B_i < \gamma_1\} \cup \{A_i < \gamma_1\} \cup \{B_i > \gamma_2\} \cup \{A_i > \gamma_2\} \\ &= \{\min(B_i, A_i) < \gamma_1\} \cup \{\max(B_i, A_i) > \gamma_2\}\end{aligned} \tag{1.8}$$

In the sequel, we note $d_i = \min(B_i, A_i)$ and $D_i = \max(B_i, A_i)$. Then we have:

$$P(Q_i = 1) \leq P(\{d_i < \gamma_1\} \cup \{D_i > \gamma_2\}), \quad i = k, \dots, n^\star. \tag{1.9}$$

This implies the following:

$$P\Big(\sum_{j=i}^{i+c-1} Q_j \geq pc\Big) \leq P\Big(\sum_{j=i}^{i+c-1} \mathbf{1}(\{d_j < \gamma_1\} \cup \{D_j > \gamma_2\}) \geq pc\Big) \tag{1.10}$$

Now, we can bound the right-hand side of Equation (1.10):

$$\begin{aligned}&P\Big(\sum_{j=i}^{i+c-1} \mathbf{1}(\{d_j < \gamma_1\} \cup \{D_j > \gamma_2\}) \geq pc\Big) \\ \leq &P\Big(\sum_{j=i}^{i+c-1} \mathbf{1}(\{d_j < \gamma_1\}) + \mathbf{1}(\{D_j > \gamma_2\}) \geq pc\Big) \\ \leq &P\Big(\sum_{j=i}^{i+c-1} \mathbf{1}(\{d_j < \gamma_1\}) \geq pc/2\Big) + P\Big(\sum_{j=i}^{i+c-1} \mathbf{1}(\{D_j > \gamma_2\}) \geq pc/2\Big)\end{aligned} \tag{1.11}$$

Then, we can express the right-hand side of Equation (1.11) as:

$$\begin{aligned}&P\Big(\sum_{j=i}^{i+c-1} \mathbf{1}(\{d_j < \gamma_1\}) \geq pc/2\Big) + P\Big(\sum_{j=i}^{i+c-1} \mathbf{1}(\{D_j > \gamma_2\}) \geq pc/2\Big) \\ = &P(d_{i(\lceil pc/2 \rceil)} < \gamma_1) + P(D_{i(c-\lceil pc/2 \rceil)} > \gamma_2)\end{aligned} \tag{1.12}$$

Finally we have:

$$
\begin{aligned}
& P(\exists i \in \{k, \dots, n^\star\}, \quad \sum_{j=i}^{i+c-1} Q_j \geq pc) \\
=& P\Big(\bigcup_{i=k}^{n^\star} \Big\{ \sum_{j=i}^{i+c-1} Q_j \geq pc \Big\}\Big) \\
\leq& P\Big(\bigcup_{i=k}^{n^\star} \Big\{ \sum_{j=i}^{i+c-1} \mathbf{1}(\{d_j < \gamma_1\}) \geq pc/2 \Big\}\Big) + P\Big(\bigcup_{i=k}^{n^\star} \Big\{ \sum_{j=i}^{i+c-1} \mathbf{1}(\{D_j > \gamma_2\}) \geq pc/2 \Big\}\Big) \qquad (1.13) \\
=& P\Big(\bigcup_{i=k}^{n^\star} \{d_{i(\lceil pc/2 \rceil)} < \gamma_1\}\Big) + P\Big(\bigcup_{i=k}^{n^\star} \{D_{i(c-\lceil pc/2 \rceil)} > \gamma_2\}\Big) \\
=& P\Big(\min_{i=k,\dots,n^\star} d_{i(\lceil pc/2 \rceil)} < \gamma_1\Big) + P\Big(\max_{i=k,\dots,n^\star} D_{i(c-\lceil pc/2 \rceil)} > \gamma_2\Big) \\
=& \frac{\alpha}{2} + \frac{\alpha}{2} = \alpha
\end{aligned}
$$

We go from line 2 to line 3 using Equations (1.10) and (1.11). We go from line 3 to line 47 using Equation (1.12). Finally, we go from line 5 to 6 using the thresholds γ_1 and γ_2 of Proposition 1. It finishes the proof. □

1.3 Monte Carlo Algorithm for Computing (γ_1, γ_2)

Input: n, k, c, p, α, V
// the length n of the trajectory
// the window size k
// the cluster parameters (c, p)
// the level $\alpha \in (0, 1)$
// the number V of Monte Carlo experiments
Result: $\hat{\gamma}_1(n, k, c, p, \alpha)$ $\hat{\gamma}_2(n, k, c, p, \alpha)$
for *i=1* **to** V **do**
  Generate $\mathbb{X}_n^i$ of size n from the null hypothesis (3.2) (see the paper) with $\sigma = 1$ and $\Delta = 1$;
  // Compute the statistics (4.1) (see the paper) along $\mathbb{X}_n^i$
  for *j=k* **to** *n-k* **do**
    Compute (B_j^i, A_j^i) from (4.1);
    Set $d_j^i = \min(B_j^i, A_j^i)$;
    Set $D_j^i = \max(B_j^i, A_j^i)$;
  end
  for *r=k* **to** *n-k-c+1* **do**
    Compute s_r^i the $\lceil pc \rceil$ smallest element of $(d_r^i, \ldots, d_{r+c-1}^i)$;
    Compute S_r^i the $c - \lceil pc \rceil$ smallest element of $(d_r^i, \ldots, d_{r+c-1}^i)$;
  end
  Compute $m_i = \min_r(S_r^i)$ and $M_i = \max_r(s_r^i)$;
end
Let $(\tilde{m}_1, \ldots, \tilde{m}_V)$ the sorted m_is and $(\tilde{M}_1, \ldots, \tilde{M}_V)$ the sorted M_is;
Set $\hat{\gamma}_1(n, k, \alpha) = \tilde{m}_{\lfloor (\alpha/2)V \rfloor}$ and $\hat{\gamma}_2(n, k, \alpha) = \tilde{M}_{\lfloor (1-\alpha/2)V \rfloor}$;

Algorithm 1: Estimation of the cut-off values $\tilde{\gamma}_1$ and $\tilde{\gamma}_2$ by Monte Carlo simulations. For estimating $(\gamma_1^\star, \gamma_2^\star)$, one should turn pc into $pc/2$ in this algorithm.

2 Choice of the Parameter (c, p) in the Aggregated Procedure 1

A cluster of candidate change-points (Step 2 of Procedure 1) is defined as a subset of successive indexes $\mathcal{M}$ such that, for all subsets of size c of successive indexes of $\mathcal{M}$, the proportion of candidate change-points is larger than the proportion p. Then the selection of the segment of the trajectory where a change-point is detected is very dependent on the choice of the parameter (c, p). As discussed in Section 4.1 of the paper, it is natural to choose a value p in the interval $(1/2, 1)$ and a value of c smaller than the size k of subtrajectories. Based on these ideas, we carried a sensivity analysis on parameter (c, p) on the simulation schemes described in Table 2 of the paper. The results are summarized in Table 3. The choice $(c, p) = (k/2, 0.75)$ appears to be a good compromise to detect the right number of change-points across the different scenario. In fact, over all the simulation schemes, this choice has the best ($e.g$ lowest) mean rank in terms of percentages of trajectories detected with the right number of change-points.

3 Other Simulation Results

In this section we present some others results on simulation.

3.1 Change in Parameter Values for a Fixed Type of Motion In this subsection, we study the performance of our approach for detecting changes in parameter values for a fixed type of motion. Monnier et al. (2015) consider this case in Model 3 and 5, see Section 6.2 of the paper. Table 5 shows that our procedure do not detect the change-points for Scenario 7 (Table 4) since the percentage of detections is around the type I error rate $\alpha = 5\%$ whatever the scale of changes in the diffusion coefficient for Brownian motion. Such result was expected as the distribution of the test statistic do not depend on the diffusion coefficient σ under Brownian motion. In other words, our procedure will detect with probability $(1-\alpha)$ the trajectory as Brownian even if the diffusion coefficient switches over time.
If such changes have to be explored, we recommend : i/ to apply our procedure in order to detect if the trajectory is fully Brownian (or even if it exists a Brownian subtrajectory long-enough); ii/ to use a specific procedure which takes into account such changes in their model, as in Monnier et al. (2015), Yin et al. (2018) or standard statistical change-points techniques (see for example Killick & Eckley (2014)) which detects switching of diffusion coefficient.

	Brownian with drift				Ornstein-Uhlenbeck				
$(c/k, p)$	$v = 0.6$	$v = 0.8$	$v = 1$	$v = 2$	$\lambda = 1$	$\lambda = 2$	$\lambda = 3$	$\lambda = 4$	Mean Rank
(0.25,0.5)	10	13	9	13	14	15	14	14	12.75
(0.25,0.6)	16	15	16	15	18	16	17	17	16.25
(0.25,0.7)	17	17	18	18	16	19	18	19	17.75
(0.25,0.75)	20	20	21	20	19	21	21	21	20.375
(0.25,0.80)	23	22	22	22	22	22	22	23	22.25
(0.25,0.9)	25	24	25	25	24	24	24	24	24.375
(0.25,1)	26	26	26	26	25	25	27	27	26.00
(0.5,0.5)	14	12	13	11	4	6	4	4	8.50
(0.5, 0.6)	9	8	7	8	6	7	7	7	7.375
(0.5,0.7)	5	4	4	5	5	10	10	10	6.625
(0.5,0.75)	**2**	**3**	**3**	**2**	**7**	**12**	**11**	**12**	**6.50**
(0.5, 0.8)	4	5	5	3	9	13	15	15	8.625
(0.5,0.9)	6	7	8	7	15	18	19	18	12.25
(0.5,1)	8	9	11	9	23	23	23	22	16.00
(0.75,0.5)	22	23	23	23	3	1	1	1	12.125
(0.75,0.6)	18	18	17	17	1	2	2	2	9.625
(0.75,0.7)	11	11	10	10	2	3	3	6	7.00
(0.75,0.75)	7	6	6	6	8	8	9	9	7.375
(0.75,0.8)	3	2	2	4	11	9	12	11	6.75
(0.75,0.9)	1	1	1	1	20	20	20	20	10.50
(0.75,1)	12	10	12	12	26	26	26	26	18.75
(1,0.5)	27	27	27	27	12	4	6	3	16.625
(1,0.6)	24	25	24	24	10	5	5	5	15.25
(1,0.7)	19	21	19	19	13	11	8	8	14.75
(1,0.75)	15	16	15	16	17	14	13	13	14.875
(1,0.8)	13	14	14	14	21	17	16	16	15.625
(1,0.9)	21	19	20	21	27	27	25	25	23.125
(1,1)	28	28	28	28	28	28	28	28	28.00

Table 3: Ranks of the performances of the aggregated Procedure 1 according to the pair values $(c/k, p)$ and the simulation scenario (see Table 2 of the paper). The ranks are computed from 1 001 trajectories of length $n = 300$ for each simulation scenario. We use the aggregated Procedure 1 with window sizes $(20, 30, 40)$. For each pair $(c/k, p)$, and for each simulation scenario, we compute the percentage of trajectories for which we detect the right number of change-points. Then, for a fixed simulation scenario, we rank the pairs $(c/k, p)$ according to this criterion. The last column averages all the ranks over the different scenarios. The pair $(c/k, p)$ with the lowest mean rank is highlighted in bold.

Table 4: Simulation scenario for changes in diffusion coefficient for Brownian motion

Times	Scenario 7
$[1, 75]$	Brownian motion with $\sigma_1 = 1$
$[76, 150]$	Brownian motion with $\sigma_2 \neq 1$

Table 5: Estimated probability of detecting a change-point with Procedure 1 in Scenario 7 (Table 4) over 1 001 Brownian trajectories and for different window sizes k.

	Diffusion coefficient σ_2			
k	2	5	10	100
20	4.2	5.9	4.7	5.5
30	5.9	4.3	5.6	5.5
40	5.8	5.1	5.7	6.5

3.2 Comparisons with Competitive Methods Table 6 and 7 assess the method of Vega et al. (2018) on scenario 1 and 2 (see Table 2 of the paper). Our method outperforms Vega et al. (2018) in all cases suggesting that the choice of the thresholds of the MSS-slopes depend very much on the models chosen for calibration.

Table 6: Performance of the method of Vega et al. (2018) for Scenario 2 (see Table 2 of the paper) for different values of parameter v over 1 001 simulated trajectories.

	$\hat{N} - N$						
λ	-2	-1	0	1	≥ 2	τ_1	τ_2
1	29.8	5.2	46.2	11.3	7.6	102.9 (36.9)	181.8 (31)
2	17.8	3.7	56.7	14.2	7.6	102.5 (26.7)	175.1 (23.7)
3	12.7	1	63.2	16.5	6.6	104.5 (19.2)	174.6 (15.9)
4	6.3	1.1	68.1	16.9	7.6	103.5 (16.9)	173.4 (16.4)

Table 7: Performance of the method of Vega et al. (2018) for Scenario 1 (see Table 2) for different values of parameter v.

	$\hat{N} - N$						
v	-2	-1	0	1	≥ 2	τ_1	τ_2
0.6	14.8	7.7	47.9	13.5	16.2	97.1 (38.7)	180.5 (37.5)
0.8	0.7	8.9	63.3	14.6	12.5	93.3 (27.4)	188.7 (31.2)
1	0.3	5.8	67.9	15.6	10.4	90.5 (23.2)	187.5 (27.1)
2	0	3.3	78.6	12.7	5.4	93.9 (13.7)	181 (12.6)

4 Alternative Testing Strategy

As mentioned in Section 4.1 of the paper, we carry $2(n - 2k + 2)$ tests, testing if the backward trajectory and forward trajectory starting at t_i $i = k, \ldots, n - k$ are Brownian or superdiffusive/subdiffusive. Then, we proposed a test procedure that controls the type I error at level α : when the trajectory is fully Brownian, we falsely detect a change-point with probability α.

In this context of multiple tests, a natural idea is to use the Benjamini & Hochberg (1995) method that controls another error rate at level α, namely the false discovery rate. In our case, due to the overlapping of the tested subtrajectories, the tests are correlated. In such a situation, Benjamini et al. (2001) propose a modification of the original procedure of Benjamini & Hochberg (1995). Specifically, they modify the threshold of the procedure of Benjamini & Hochberg (1995) originally set to α. Instead they use the threshold $\alpha / \sum_{i=1}^{m} 1/i$, m denoting the number of tests.

However, in our case the interpretation of the false discovery rate is not clear. In fact, the tested subtrajectories containing a true change-point are a mix of Brownian, superdiffusion or superdiffusion. Then, for these subtrajectories, none of the hypothesises of the test (H_{0i} : Brownian, H_{1i} subdiffusive or H_{2i} superdiffusive) is true. Therefore, we can not define the false discovery rate which is based on the numbers of misclassified hypothesises.

Nevertheless, the procedure could provide satisfying results even without this interpretation. Then, we implement the Benjamini & Hochberg (1995) procedure in our method. As we deal with three-decision test, we use the extension of the Benjamini & Hochberg (1995) proposed in (Briane et al. 2018, Sec. IV). The step 1(b) of Procedure 1 is replaced by the modified Benjamini & Hochberg (1995) procedure for three-decision test. We can carry the aggregation strategy as for the original Procedure 1.

The performances of the aggregated Procedure 1 with the Benjamini & Hochberg (1995)

Table 8: Performance of the aggregated Procedure 1 with the Benjamini & Hochberg (1995) step on the Scenario 1 (see Table 2 of the paper) for different values of parameter v.

Threshold	v	$\hat{N}-N$ -2	-1	0	1	≥ 2	τ_1	τ_2
α	0.6	24.0	6.9	64.5	1.4	3.2	113.2 (14.8)	165.2 (15.4)
	0.8	1.6	3.1	84.7	2.0	8.6	108.5 (11.4)	169.6 (11.2)
	1	0.1	2.1	88.7	2.2	6.9	104.4 (7.5)	172.8 (7.1)
	2	0.0	2.3	92.7	1.8	3.2	101.3 (3.6)	176.0 (5.1)
$\alpha \sum_{i=1}^{m} 1/i$	0.6	57.0	5.3	36.5	0.8	0.4	115.4 (14.6)	163.2 (15.3)
	0.8	10.1	6.9	79.6	0.4	3.0	109.9 (11.9)	167.8 (11.5)
	1	0.4	4.0	89.0	2.0	4.6	105.3 (7.6)	172.4 (7.1)
	2	0.0	3.5	95.6	0.5	0.4	101.4 (2.7)	175.7 (2.5)

step on the simulation scheme 1 (see Section 5.2) are shown in Table 8 and Table 9. We aggregate the detections of the window sizes $(20, 30, 40)$ using $n_{\min} = 10$. We compute the performances for the original procedure of Benjamini & Hochberg (1995) (threshold set to α) and for the modified procedure of Benjamini et al. (2001) which takes into account the correlations between the tests (threshold set to $\alpha / \sum_{i=1}^{m} 1/i$).

Actually, the results are significantly worse than with our original algorithm when we use the modified threshold $\alpha / \sum_{i=1}^{m} 1/i$ (here the number of tests is $m = 2(n - 2k + 2)$) on both simulation scenario (Table 8 and Table 9). When we use the original threshold α (which does not take into account the correlation between tests), we got better results. The performances are still always worse than with our original algorithm. Note that when we use the Benjamini & Hochberg (1995) procedure in our algorithm, it is also more time consuming (166 sec for 1 001 trajectories from the simulation scheme 1) than the original version of our algorithm (99 sec for 1 001 trajectories from the simulation scheme 1). It is due to the fact that we have to estimate the p-values in the Benjamini & Hochberg (1995) procedure.

Table 9: Performance of the aggregated Procedure 1 with the Benjamini & Hochberg (1995) step on the Scenario 2 (see Table 2 of the paper) for different values of parameter v.

Threshold	λ	$\hat{N}-N$ -2	-1	0	1	≥ 2	τ_1	τ_2
α	1	17.8	5.6	73.6	1.7	1.3	107.8 (11.5)	167.4 (10.9)
	2	3.7	4.9	84.9	2.7	3.8	109.0 (9.2)	167.4 (8.9)
	3	2.0	5.3	85.7	3.3	3.7	110.0 (9.4)	166.9 (9.2)
	4	2.4	6.0	84.3	3.2	4.1	110.6 (8.8)	166.0 (8.6)
$\alpha\sum_{i=1}^{m} 1/i$	1	75.2	4.8	19.9	0.1	0.0	110.5 (10.7)	163.8 (11.7)
	2	25.9	6.8	66.9	0.4	0.0	112.4 (11.1)	164.4 (10.4)
	3	21.4	6.6	70.5	1.4	0.1	112.8 (10.4)	164.0 (10.0)
	4	22.8	7.1	68.7	1.3	0.1	112.8 (10.7)	163.3 (10.0)

5 Supplementary Figures

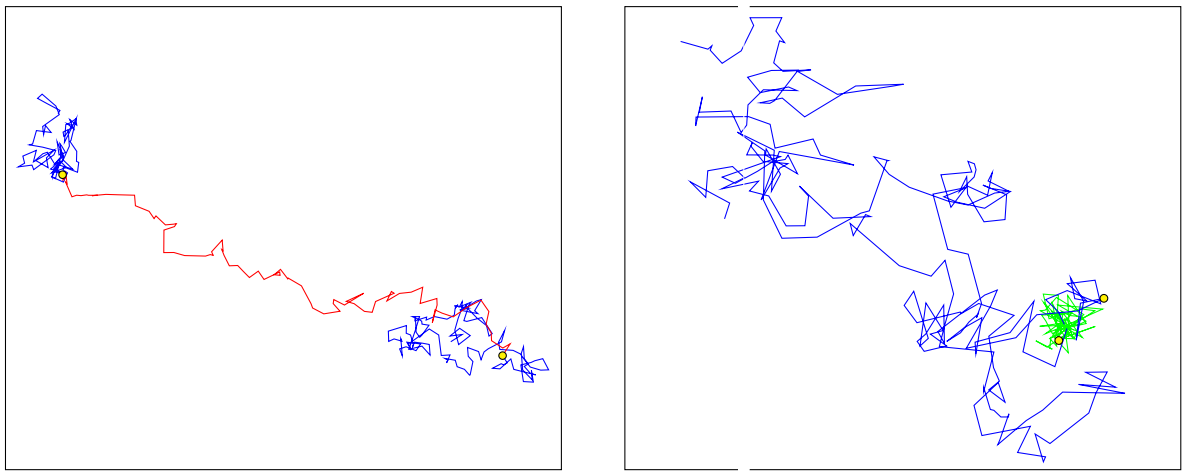

Figure 1: Simulated trajectories from Scenario 1 (left) with $v = 0.8$ and from Scenario 2 with $\lambda = 1$ (right). Two change-points $\hat{N} = 2$ (yellow dots) are respectively detected at $(\hat{\tau}_1, \hat{\tau}_2) = (89, 172)$ (on left) and $(\hat{\tau}_1, \hat{\tau}_2) = (87, 165)$ (on right) with Procedure 1 and $k = 30$.

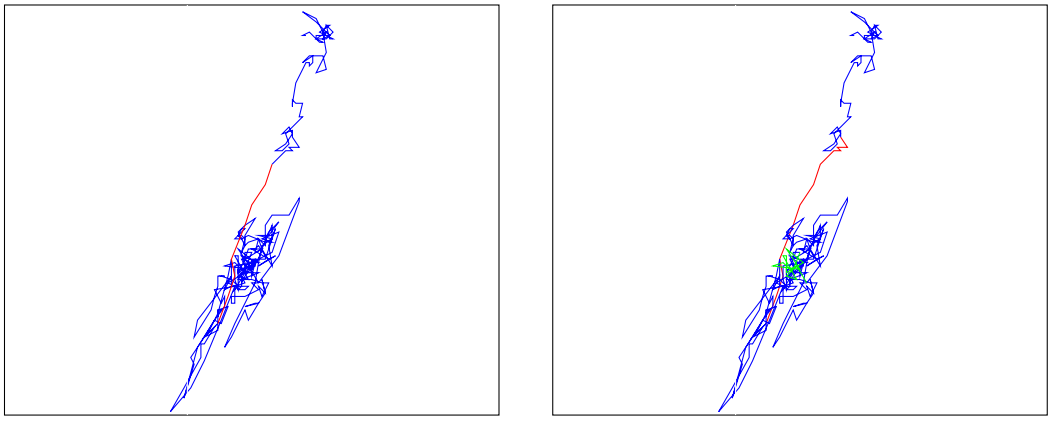

$k = 10$ $k = 15$

Figure 2: β-actin mRNP trajectory analysed with the Procedure 1 with window size $k = 10$ (left) and $k = 15$ (right). The detected change-points are $\boldsymbol{\tau} = (67, 75)$ for $k = 10$; the motion alternates between Brownian, superdiffusion and Brownian. The detected change-points are $\boldsymbol{\tau} = (62, 75, 282)$ for $k = 15$; the motion alternates between Brownian motion, superdiffusion, Brownian motion and finally subdiffusion. The motion type of the sub-trajectories is depicted in blue for Brownian, in red for superdiffusion, and in green for subdiffusion.

References

Benjamini, Y. & Hochberg, Y. (1995), 'Controlling the false discovery rate: a practical and powerful approach to multiple testing', *Journal of the Royal statistical society: series B (Methodological)* **57**(1), 289–300.

Benjamini, Y., Yekutieli, D. et al. (2001), 'The control of the false discovery rate in multiple testing under dependency', *The annals of statistics* **29**(4), 1165–1188.

Briane, V., Kervrann, C. & Vimond, M. (2018), 'Statistical analysis of particle trajectories in living cells', *Phys. Review E* **97**(6), 062121.

Killick, R. & Eckley, I. (2014), 'changepoint: An r package for changepoint analysis', *Journal of statistical software* **58**(3), 1–19.

Mishura, Y. (2008), *Stochastic calculus for fractional Brownian motion and related processes*, Vol. 1929, Springer Science & Business Media.

Monnier, N., Barry, Z., Park, H. Y., Su, K.-C., Katz, Z., English, B. P., Dey, A., Pan, K., Cheeseman, I. M., Singer, R. H. et al. (2015), 'Inferring transient particle transport dynamics in live cells', *Nature Meth.* **12**(9), 838–840.

Nualart, D. & Ouknine, Y. (2002), 'Regularization of differential equations by fractional noise', *Stochastic Processes and their Applications* **102**(1), 103–116.

Vega, A. R., Freeman, S. A., Grinstein, S. & Jaqaman, K. (2018), 'Multistep track segmentation and motion classification for transient mobility analysis', *Biophysical journal* **114**(5), 1018–1025.

Yin, S., Song, N. & Yang, H. (2018), 'Detection of velocity and diffusion coefficient change points in single-particle trajectories', *Biophysical journal* **115**(2), 217–229.